

* now at: Department of Ecology, College of Urban and Environmental Science, Peking University, China

Received: 11 May 2010 – Accepted: 15 July 2010 – Published: 29 July 2010

Correspondence to: L. Feng (lfeng@staffmail.ed.ac.uk)

Published by Copernicus Publications on behalf of the European Geosciences Union.

ACPD

10, 18025–18061, 2010

GEOS-Chem CO₂ simulation

L. Feng et al.

Title Page

Abstract

Introduction

Conclusions

References

Tables

Figures

⏪

⏩

◀

▶

Back

Close

Full Screen / Esc

Printer-friendly Version

Interactive Discussion



Abstract

We evaluate the GEOS-Chem atmospheric transport model (v8-02-01) of CO₂ over 2003–2006, driven by GEOS-4 and GEOS-5 meteorology from the NASA Goddard Global Modelling and Assimilation Office, using surface, aircraft and space-borne concentration measurements of CO₂. We use an established ensemble Kalman filter to estimate a posteriori biospheric+biomass burning (BS+BB) and oceanic (OC) CO₂ fluxes from 22 geographical regions, following the TransCom 3 protocol, using boundary layer CO₂ data from a subset of GLOBALVIEW surface sites. Global annual net BS+BB+OC CO₂ fluxes over 2004–2006 for GEOS-4 (GEOS-5) meteorology are -4.4 ± 0.9 (-4.2 ± 0.9), -3.9 ± 0.9 (-4.5 ± 0.9), and -5.2 ± 0.9 (-4.9 ± 0.9) Pg C yr⁻¹, respectively. The regional a posteriori fluxes are broadly consistent in the sign and magnitude of the TransCom-3 study for 1992–1996, but we find larger net sinks over northern and southern continents. We find large departures from our a priori over Europe during summer 2003, over temperate Eurasia during 2004, and over North America during 2005, reflecting an incomplete description of terrestrial carbon dynamics. We find GEOS-4 (GEOS-5) a posteriori CO₂ concentrations reproduce the observed surface trend of 1.91–2.43 ppm yr⁻¹, depending on latitude, within 0.15 ppm yr⁻¹ (0.2 ppm yr⁻¹) and the seasonal cycle within 0.2 ppm (0.2 ppm) at all latitudes. We find the a posteriori model reproduces the aircraft vertical profile measurements of CO₂ over North America and Siberia generally within 1.5 ppm in the free and upper troposphere but can be biased by up to 4–5 ppm in the boundary layer at the start and end of the growing season. The model has a small negative bias in the free troposphere CO₂ trend (1.95–2.19 ppm yr⁻¹) compared to AIRS data which has a trend of 2.21–2.63 ppm yr⁻¹ during 2004–2006, consistent with surface data. Model CO₂ concentrations in the upper troposphere, evaluated using CONTRAIL (Comprehensive Observation Network for TRace gases by AirLiner) aircraft measurements, reproduce the magnitude and phase of the seasonal cycle of CO₂ in both hemispheres. We generally find that the GEOS meteorology reproduces much of the observed tropospheric CO₂ variability,

GEOS-Chem CO₂ simulation

L. Feng et al.

Title Page

Abstract

Introduction

Conclusions

References

Tables

Figures

◀

▶

◀

▶

Back

Close

Full Screen / Esc

Printer-friendly Version

Interactive Discussion



suggesting that these meteorological fields will help make significant progress in understanding carbon fluxes as more data become available.

1 Introduction

Atmospheric transport models have played a central role in the interpretation of atmospheric CO₂ concentrations. They have been used in the forward mode to assess whether a priori flux inventories can reproduce observed atmospheric CO₂ concentration variations (e.g., Gurney et al., 2003), and in the inverse mode to adjust surface CO₂ fluxes in order to minimize the discrepancy between observed and model concentrations (e.g., Gurney et al., 2002, 2004; Rödenbeck et al., 2003; Stephens et al., 2007). Model evaluation is therefore a critical step in developing robust flux estimates using the inverse model.

A substantial amount of previous work involved with assessing atmospheric transport models of CO₂ has been coordinated by the atmospheric tracer transport model intercomparison project (TransCom, e.g., Gurney et al., 2003, 2004). They have in particular assessed the sensitivity of CO₂ flux estimation to atmospheric transport by quantifying the variation from several independent transport models. Up until now, the GEOS-Chem global 3-D transport model has not participated in this project, however, the model has been extensively evaluated using a wide range of ground-based, aircraft, and satellite measurements of CO₂, CO, HCN, CH₃CN (e.g., Li et al., 2003, 2009; Heald et al., 2004; Palmer et al., 2008).

Previous work attempted to evaluate the GEOS-Chem model using the SCanning Imaging Absorption SpectroMeter for Atmospheric CHartography (SCIAMACHY) CO₂ columns from 2003 but the results were inconclusive because there was also substantial unexplained bias in the satellite data (Palmer et al., 2008). Within that study, we performed a limited evaluation of model CO₂ columns at Park Falls, USA, and found that the model could not reproduce the magnitude of the minima during the growing season, consistent with previous studies (Yang et al., 2007). We also showed that

GEOS-Chem CO₂ simulation

L. Feng et al.

Title Page

Abstract

Introduction

Conclusions

References

Tables

Figures

◀

▶

◀

▶

Back

Close

Full Screen / Esc

Printer-friendly Version

Interactive Discussion



**GEOS-Chem CO₂
simulation**

L. Feng et al.

[Title Page](#)[Abstract](#)[Introduction](#)[Conclusions](#)[References](#)[Tables](#)[Figures](#)[◀](#)[▶](#)[◀](#)[▶](#)[Back](#)[Close](#)[Full Screen / Esc](#)[Printer-friendly Version](#)[Interactive Discussion](#)

the model reproduced GLOBALVIEW surface concentration data over North America. A preliminary study using data from the 2003 CO₂ Budget and Rectification Airborne experiment (COBRA) (Bakwin et al., 2003) showed that the model had a positive bias of 2 ± 3.5 ppm throughout the boundary layer, suggesting too weak model vertical mixing; a relatively small model bias in the free troposphere (2–6 km) where surface flux signatures are relatively weak, increasing to a positive bias of 2.3 ± 1.8 ppm at 8–10 km that was attributed to a possible error in describing stratosphere troposphere exchange (Shia et al., 2006).

Here, we perform a more comprehensive evaluation of the GEOS-Chem global 3-D transport model simulation of CO₂ during 2003–2006 using surface, aircraft and satellite data that span the depth of the troposphere. We are especially looking for unexplained biases that could compromise the ability of this model to inform the carbon cycle community on changes in the magnitude and distribution of CO₂ sources and sinks. In Sect. 2, we describe the GEOS-Chem model and the surface flux inventories. In Sect. 3, we describe the ground-based, aircraft and satellite data we use to evaluate model CO₂ concentrations, and to infer the magnitude and distribution of surface sources and sinks. In Sect. 4, we describe the ensemble Kalman filter, which is used to optimally fit surface fluxes to minimize the discrepancy between observed and model ground-based data. We present in Sect. 5 the a posteriori flux estimates for the terrestrial biosphere and biomass burning, and ocean biosphere from 2003–2006. In Sect. 6 we evaluate the model, driven by a priori and a posteriori flux estimates, using surface, aircraft and satellite data that focus on the boundary layer, free troposphere, and upper troposphere. We conclude the paper in Sect. 7.

2 The GEOS-Chem model of atmospheric CO₂

We use the GEOS-Chem global 3-D chemistry transport model (v8-02-01) to relate prescribed CO₂ surface fluxes to atmospheric CO₂ concentrations, driven separately by GEOS-4 (Bloom et al., 2005) and GEOS-5 (Rienecker et al., 2008) assimilated

meteorology data from the Global Modeling and Assimilation Office Global Circulation Model based at NASA Goddard Space Flight Center. The resulting model calculations using GEOS-4 and GEOS-5 meteorology are denoted as G4 and G5, respectively.

Using different meteorological fields offers us an opportunity to test the sensitivity of our results to differences in atmospheric transport. These 3-D meteorological data are updated every 6 h, and the mixing depths and surface fields are updated every 3 h. We use these data at a horizontal resolution of 2° latitude \times 2.5° longitude. GEOS-4 (GEOS-5) meteorology has 30 (47) hybrid vertical levels ranging from the surface to the mesosphere, 20 (30) of which are below 12 km.

We use a version of the GEOS-Chem transport model that accounts for CO_2 concentration contributions from geographical regions to the total atmospheric concentration. Figure 1 shows the 22 geographical regions we consider, which are based on the TransCom-3 (T3) study (Gurney et al., 2002). The CO_2 simulation is based on previous work (Suntharalingam et al., 2005; Palmer et al., 2006, 2008) with updates described below. We include a priori surface estimates for fossil fuel, biofuel, biomass burning, and surface fluxes from the ocean and terrestrial biospheres. We use a spatial pattern of annual fossil fuel emissions based on work for 1995 (Suntharalingam et al., 2005), and scale fluxes to 2003–2006 based on global total fossil fuel emissions, including emissions from the top 20 emitting countries, from the Carbon Dioxide Information Analysis Centre (Marland et al., 2007). Resulting annual global fossil fuel emissions are 7.29, 7.67, 7.97, and 8.23 Pg C for the year 2003 to 2006, respectively. We ignore temporal variation of fossil fuel emission on timescales less than a year. Other studies show that including this additional temporal variability can be important but associated uncertainties are substantial (Erickson et al., 2008). We use climatological biofuel emission estimates (Yevich and Logan, 2003). Monthly biomass burning emissions are taken from the second version of the Global Fire Emission Database (GFEDv2) for 2003–2006 (van der Werf et al., 2006), which are derived from ground-based and satellite observations of land-surface properties. We prescribe monthly ocean fluxes that have been determined from sea-surface $p\text{CO}_2$ observations (Taka-

**GEOS-Chem CO_2
simulation**

L. Feng et al.

[Title Page](#)[Abstract](#)[Introduction](#)[Conclusions](#)[References](#)[Tables](#)[Figures](#)[◀](#)[▶](#)[◀](#)[▶](#)[Back](#)[Close](#)[Full Screen / Esc](#)[Printer-friendly Version](#)[Interactive Discussion](#)

hashi et al., 2009). These newly available estimates have an annual net uptake of 1.4 PgC. We use the CASA biosphere model (Randerson et al., 1997) constrained by observed GEOS meteorology and Normalized Difference Vegetation Index (NDVI) data to prescribe atmospheric CO₂ exchange with the terrestrial biosphere. CASA is spun up for several hundred years using the multi-annual mean monthly meteorology and NDVI for the simulation period. This results in a nearly annually-balanced biosphere. Specific monthly CASA fluxes are derived using monthly weather and NDVI data with variations on shorter timescales determined by 3-h G4/G5 meteorology analyses (Olsen and Randerson, 2004). This produces flux distributions with diurnal to interannual variability, but no long-term trend and a mean annual net flux very near zero.

We initialise our model run on January 2002 using a previous model run (Palmer et al., 2006), which we integrate forward to January 2003. Due to the availability of GEOS-5 meteorology data, the initial G5 CO₂ distribution on 1 January 2004 is constructed from the G4 model simulation that starts from January 2003. We include an additional initialization to correct for the model bias introduced by not accounting for the net uptake of CO₂ from the terrestrial biosphere. We make this downward correct by comparing the difference between GLOBALVIEW CO₂ data (GLOBALVIEW-CO₂) and model concentrations over the Pacific during January 2003. Differences range from 1 to 4 ppm with a median of 3.5 ppm, and we subtract this value globally, following Suntharalingam et al. (2005).

3 Data used to infer CO₂ flux estimates and to evaluate GEOS-Chem

We use independent data to estimate surface fluxes and to evaluate resulting model atmospheric CO₂ concentrations.

GEOS-Chem CO₂ simulation

L. Feng et al.

Title Page

Abstract

Introduction

Conclusions

References

Tables

Figures

◀

▶

◀

▶

Back

Close

Full Screen / Esc

Printer-friendly Version

Interactive Discussion



3.1 GLOBALVIEW CO₂ data

We use the GLOBALVIEW smoothed CO₂ data set to infer surface CO₂ flux estimates. This is a pseudo dataset, representing a (smooth) statistical fit to flask and continuous CO₂ data from a global ground-based network of over 200 stations. The smoothed values are extracted from a curve fitted to measurements that are thought to represent large well-mixed air parcels. GLOBALVIEW also provides extended dataset with 48 pseudo-weekly synchronous CO₂ values per year from an extrapolation procedure used to fill gaps in the observation record at individual sites (Masarie and Tans, 1995).

Figure 1 shows the geographical of the available 277 stations during the time period 2003–2006. Nearly one-third of available stations are located around North America and Europe, with little coverage over the tropics. We sample the model at the nearest grid box to the station location and average the data over 48 pseudo weeks. For stations that straddle ocean/land model grid boxes we sample the model at the nearest windward ocean grid boxes, as suggested by the TransCom 3 protocol (Gurney et al., 2003).

3.2 Aircraft data

To help evaluate the model vertical distribution of CO₂ throughout the troposphere we use aircraft data from the Comprehensive Observation Network for TRace gases by AirLiner (CONTRAIL, Matsueda et al., 2002); Intercontinental Chemical Transport Experiment North America (INTEX-NA, Singh et al., 2006); the COBRA campaign (Bakwin et al., 2003); and Airborne Extensive Regional Observations in SIBeria (YAK-AEROSIB, Paris et al., 2008, 2010). Table 1 provides a summary of these campaigns; for the sake of brevity, we refer the reader to the dedicated campaign literature, as cited above, for further details of each dataset. We sample the model at the appropriate time and location of each observation.

Title Page

Abstract

Introduction

Conclusions

References

Tables

Figures

◀

▶

◀

▶

Back

Close

Full Screen / Esc

Printer-friendly Version

Interactive Discussion



3.3 Atmospheric infrared sounder satellite data

The Atmospheric Infrared Sounder (AIRS), aboard the NASA Aqua satellite, was launched into a sun-synchronous near-polar orbit in 2002. AIRS measures atmospheric thermal infrared radiation between 3.74 μm and 15.4 μm using 2378 channels.

CO₂ columns are retrieved from selected CO₂ channels in the 15 μm band using the Vanishing Partial Derivatives (VPD) algorithm, which does not rely on a priori information (Chahine et al., 2008). These thermal IR channels are most sensitive to CO₂ at 450 hPa, with full-width half peak spanning 200–700 hPa. The horizontal resolution of the AIRS CO₂ data is 90×90 km². Previous work has shown the retrieved mid-tropospheric AIRS CO₂ data are within 2 ppm of aircraft measurements at 8–13 km (Chahine et al., 2008). We use the gridded monthly mean level-3 AIR CO₂ product. For each gridded AIRS measurement, we sample the model at the nearest 2°×2.5° grid box, convolve the resulting vertical profile with the AIRS averaging kernels that account for the vertical sensitivity of the instrument for the appropriate latitudes bin (Chahine et al., 2008), and calculate the monthly mean. The AIRS CO₂ global trend, determined by a linear least-squares fit to monthly means described using 2° latitude bins over 60° S–60° N from January 2003 to December 2008, is 2.02±0.08 ppm yr⁻¹.

4 The Ensemble Kalman Filter inverse model

We optimally fit prescribed a priori surface fluxes $S^0(x, y, t)$, via the GEOS-Chem forward model, to observed ground-based GLOBALVIEW CO₂ data at selected stations (denoted by white circles and red triangles in Fig. 1), similar to the T3 study (Gurney et al., 2002). A priori surface fluxes include those from combustion of fossil (FF) and bio- (BF) fuels, biomass burning (BB), and the terrestrial (BS) and ocean (OC)

Title Page

Abstract

Introduction

Conclusions

References

Tables

Figures

◀

▶

◀

▶

Back

Close

Full Screen / Esc

Printer-friendly Version

Interactive Discussion



biospheres (Sect. 2). The adjustment is in the following form:

$$S(x, y, t) = S^0(x, y, t) + \sum_m \sum_{i=1}^{22} \lambda_m^i \Gamma_m^i(x, y), \quad (1)$$

where each monthly basis function $\Gamma_m^i(x, y)$ represents a pulsed emission of 1 Pg C yr⁻¹ from each of the 22 individual T3 regions i during month m . For ocean regions, we assume $\Gamma_m^i(x, y)$ has a uniform spatial distribution. For land regions, the spatial distribution is informed by net primary production from the CASA model (Gurney et al., 2003, 2008). We use an Ensemble Kalman Filter (EnKF) (Feng et al., 2009) to estimate coefficients λ_m^i , which we assume have initial values of zero.

The state vector \mathbf{x} are monthly values of λ_m^i for each T3 region (Fig. 1). We evaluate the resulting a posteriori surface fluxes, S . For the purpose of this calculation we assume perfect knowledge of FF and BF, and report BS+BB and OC flux estimates; in practice, any adjustment to λ_m^i will also reflect errors in FF and BF. We express our a posteriori monthly flux estimates as the equivalent annual flux (Pg C yr⁻¹), following Gurney et al. (2004, 2008); for clarity, we also present our results as Pg C month⁻¹. For the EnKF, uncertainties associated with λ_m^i are represented by an ensemble of perturbations states $\Delta\mathbf{X}$ so that the a priori error covariance matrix \mathbf{P} is approximated by: $\mathbf{P} = \Delta\mathbf{X}(\Delta\mathbf{X})^T$. We use the full matrix representation of the EnKF, i.e., using an ensemble of the same size of the state vector dimension. The perturbation states are projected into the observation space as the perturbations to the mean atmospheric CO₂ concentrations by using the GEOS-Chem 3-D atmospheric transport model. To reduce computational costs, we introduce a lag window of 8 months to reduce the number of variables (and hence the size of ensemble) to estimate at each assimilation step. The current lag window is longer than we adopted previously for assimilating satellite measurements, reflecting the sparse spatial coverage of ground-based data. As a result, at each assimilation step of one month, we need to estimate 176 values (8 months×22 regions) of λ_m^i .

GEOS-Chem CO₂
simulation

L. Feng et al.

Title Page

Abstract

Introduction

Conclusions

References

Tables

Figures

◀

▶

◀

▶

Back

Close

Full Screen / Esc

Printer-friendly Version

Interactive Discussion



We optimally estimate the a posteriori state vector \mathbf{x}^a using:

$$\mathbf{x}^a = \mathbf{x}^f + \mathbf{K}_e[\mathbf{y}_{\text{obs}} - H(\mathbf{x}^f)], \quad (2)$$

where \mathbf{x}^f and \mathbf{x}^a are the a priori and a posteriori state vectors; the observation vectors, \mathbf{y}_{obs} , represents the atmospheric CO₂ concentrations (ppm); $H(\mathbf{x}^f)$ are the model observations (ppm), where H is the observation operator that describes the relationship between the state vector and the observations. H includes global atmospheric CO₂ transport and surface emission/sink during each assimilation lag window, and interpolation of the resulting 3-D CO₂ fields to the observation locations. We calculate the ensemble gain matrix \mathbf{K}_e (ppm⁻¹) using:

$$\mathbf{K}_e = \Delta\mathbf{X}^f(\Delta\mathbf{Y})^T[\Delta\mathbf{Y}(\Delta\mathbf{Y})^T + \mathbf{R}]^{-1}, \quad (3)$$

where \mathbf{R} is the observation error covariance, and $\Delta\mathbf{Y}$ is defined as $\Delta\mathbf{Y}=H(\Delta\mathbf{X}^f)$. To calculate $\Delta\mathbf{Y}$, we introduce model tracers to describe the perturbation of surface fluxes, $\Delta\mathbf{X}$, on the variability of observed CO₂ concentrations (Palmer et al., 2006, 2008).

We assume an a priori uncertainty c_m^i for values of λ_m^i over land region i to

be $c_m^i = 0.5\sqrt{1.0 + \left(\overline{BS_m^i}\right)^2}$, where $\overline{BS_m^i}$ represents the monthly BS flux (Pg C yr⁻¹);

adding 1.0 avoids artificially small uncertainties where the prior BS flux is weak. The resulting uncertainty for each regional land surface flux is close to 50% of the a priori estimate, similar to values used in previous studies (see for example, Gurney et al., 2008). We find that our a posteriori flux estimates are relatively insensitive to c_m^i (not shown). We use a similar approach to describe the uncertainty of ocean regions

$c_m^i = 0.5\sqrt{0.6 + \left(\overline{OC_m^i}\right)^2}$, where $\overline{OC_m^i}$ is the monthly mean ocean surface fluxes. We

use a smaller offset value (0.6) for ocean fluxes, reflecting the smaller, less uncertain seasonal variation compared to the terrestrial fluxes.

GEOS-Chem CO₂ simulation

L. Feng et al.

Title Page

Abstract

Introduction

Conclusions

References

Tables

Figures

◀

▶

◀

▶

Back

Close

Full Screen / Esc

Printer-friendly Version

Interactive Discussion



Discussion Paper | Discussion Paper | Discussion Paper | Discussion Paper

**GEOS-Chem CO₂
simulation**

L. Feng et al.

Title Page

Abstract

Introduction

Conclusions

References

Tables

Figures

◀

▶

◀

▶

Back

Close

Full Screen / Esc

Printer-friendly Version

Interactive Discussion



The observation vector, \mathbf{y}_{obs} includes data from GLOBALVIEW stations, which are used to infer the monthly surface fluxes for 2003–2006. These stations, chosen based on the measurement availability during 2003–2006, are marked as white and red dots in Fig. 1; additional details of each station can be found at <http://www.esrl.noaa.gov/>.

5 We initially assimilated GLOBALVIEW surface data with relative weights larger than 6.0 for good continuity. But using this constraint effectively restricts the number of sites that can be used each year. In particular, during 2005 between 30 and 60° N we found only one station that met the weight criterion. We acknowledge that the constraint can be partly circumvented by using the raw data. Here, we relax the selection criteria for the
10 30–60° N latitude band and assimilate any surface data with relative weights larger than 4. We estimate an observation uncertainty for each GLOBALVIEW station by using the standard deviation of the weekly residual between observations and the fitted curve as provided by GLOBALVIEW (Gurney et al., 2004). We limit the minimum observation uncertainties to be 0.25 ppm, and also enlarge the uncertainties for co-located stations
15 (Gurney et al., 2004). To account for model transport (and representation) error, we assume an uniform 1.0 ppm uncertainty. We assume the observation and a priori errors are uncorrelated in time and space, resulting in diagonal matrices for \mathbf{P} and \mathbf{R} .

5 A posteriori continental and oceanic CO₂ fluxes

Global annual a posteriori CO₂ flux estimates over 2004–2006 for the G4 (G5) model
20 are -4.4 ± 0.9 (-4.2 ± 0.9), -3.9 ± 0.9 (-4.5 ± 0.9), and -5.2 ± 0.9 (-4.9 ± 0.9) Pg C yr⁻¹, respectively. These estimated fluxes using the G4/G5 meteorology are generally similar. However, in 2005 the G5 estimated net sink is higher than the G4 flux by 0.6 Pg C. This partly reflects a lack of high-quality surface measurements between 30° N and 60° N that are used in GLOBALVIEW, as discussed above. This discrepancy is also
25 associated with differences in model vertical transport (Stephens et al., 2007).

Figure 2 shows a priori and a posteriori fluxes over three T3 land aggregates: north continents (Boreal North America, Temperate North America, Europe, Boreal Eurasia,

5 Temperate Eurasia); tropical continents (Northern Africa, Tropical Asia, Tropical America); and south continents (Southern Africa, Australia, South America) (Gurney et al., 2003). In general, the assimilation process reduces the uncertainties associated with the estimated BS+BB surface fluxes over north continents, and to a lesser extent over the south continents; a posteriori uncertainties over the tropics are similar to the prior values. These error reductions reflect the efficacy of the constraints provided by GLOB-ALVIEW data. Resulting regional G4/G5 a posteriori fluxes follow the temporal changes of the prior, but have much stronger uptake during the boreal growing seasons.

10 Table 2 shows that our results are generally consistent with previous T3 experiments for 1992–1996 (Gurney et al., 2003). Our global annual G4 and G5 a posteriori estimates have much stronger sinks over northern continents during 2004–2006 (–3.00 and –3.65 Pg C yr⁻¹, respectively) compared to mean T3 estimates for 1992–1996, which may reflect a number of reasons: increased activity of the terrestrial biosphere, an overestimate of prescribed anthropogenic CO₂ emissions, or a negative model bias in boundary layer mixing (e.g., Stephens et al., 2007); we acknowledge that the most likely cause is due to changes in biospheric activity.

15 Figure 3 shows the a priori and a posteriori BS+BB CO₂ fluxes over continental Europe, Temperate North America, Boreal Eurasia, and Temperate Eurasia. A posteriori estimates based on G5 meteorological data show a larger sink over northern and southern extra-tropical continents during 2004–2006. The largest discrepancies are over Temperate Eurasia, where peak G4/G5 a posteriori CO₂ uptake can be more than twice the a priori value. There are also shifts (up to 1 month) in the peak CO₂ uptake periods over these regions. Over Europe and Temperate North America, the net emission during winter months is smaller than the prior values. The stronger uptake during the growing seasons and the smaller emission during the winters represent a substantial departure from the annually-balanced CASA model, and reflect possible overestimation of biospheric respiration by the CASA model (Gurney et al., 2004), and errors in the prescribed fossil fuel emissions (Erickson et al., 2008). Fluctuations in the a posteriori fluxes, leading to short periods of weak negative fluxes during winter

GEOS-Chem CO₂ simulation

L. Feng et al.

Title Page

Abstract

Introduction

Conclusions

References

Tables

Figures

◀

▶

◀

▶

Back

Close

Full Screen / Esc

Printer-friendly Version

Interactive Discussion



months, are likely to be an artifact due to errors in source attribution from a limited number of observations.

Figure 3 compares the a priori and a posteriori BS+BB CO₂ fluxes over T3 Tropical South America, Northern Africa, and Tropical Asia. Tropical land fluxes have weaker seasonal cycles than those characterized by the extratropics. The differences between a posteriori and a priori estimates (G4 and G5) are usually insignificant, reflecting the small number of observations available to constrain these continental fluxes. For example, the CASA biosphere model and GFEDv2 biomass burning emission estimates predict a net emission from Tropical America in August 2005; for that region and month in other years there is a net sink. Without additional data, we cannot comment on whether the model generates a realistic flux response to the drought conditions over the Amazon basin during 2005 (Phillips et al., 2009).

Figure 4 shows the ocean CO₂ fluxes for the corresponding period, which have been aggregated as (a) north ocean (North Pacific, Northern Ocean, North Atlantic); (b) tropical ocean (West Pacific, East Pacific, Tropical Atlantic, Tropical Indian); and (c) south ocean (South Pacific, South Atlantic, South Indian, Southern Ocean). The differences between the a posteriori and a priori annual ocean fluxes are generally less than 0.2 Pg C yr⁻¹ except over southern extra-tropical oceans where a posteriori annual fluxes have a negative bias of 0.3 (0.5) Pg C yr⁻¹. Large seasonal variations in the a posteriori aggregated south ocean flux are correlated with the observed changes in atmospheric CO₂ at southern high latitudes. We find that the data assimilation process introduces noise to the a priori values, which is due to the inability of the measurements to adequately constrain ocean fluxes. We find that G4 ocean CO₂ fluxes are lower than G5 fluxes by 0.3 Pg C yr⁻¹ over the north ocean, and also that G4 seasonal flux variations over the southern extra-tropical oceans are generally larger than G5.

**GEOS-Chem CO₂
simulation**

L. Feng et al.

Title Page

Abstract

Introduction

Conclusions

References

Tables

Figures

I◀

▶I

◀

▶

Back

Close

Full Screen / Esc

Printer-friendly Version

Interactive Discussion



6 Model evaluation

We use surface, aircraft and satellite data to help evaluate the GEOS-Chem G4 and G5 models driven by a priori and corresponding a posteriori flux estimates. First, we use the campaign-based aircraft data to help evaluate vertical profiles of CO₂ in the troposphere. Second, we use surface, aircraft, and satellite data to test how well the model can reproduce the observed seasonal cycle and trend of CO₂ from 2003 to 2006. We acknowledge some circularity in our using a selection of ground-based data to infer fluxes and then to use all stations (smoothed data) to evaluate model atmospheric concentrations resulting from the a posteriori fluxes, but this approach still provides a gross measure of the model fit to the surface data.

6.1 Vertical distribution

We use aircraft data from the CO₂ Budget and Regional Airborne Study during May–August, 2004 over North America; INTEX-NA that measured North American continental outflow during 2004; and from the YAK-AEROSIB campaign during 2006 (Table 1). For these campaigns we sample the model at the time and location of each measurement.

Figure 5 shows that the G4 and G5 models are typically within 2 ppm of the COBRA CO₂ observations in the free troposphere. Variability of model and observed boundary layer concentrations is similar in magnitude and larger compared to the free troposphere. The model is able to reproduce the sharp CO₂ vertical gradient in the boundary layer during June and July, but has a positive bias of 5 ppm in the early (May) growing season and a negative bias of 3.5 ppm in the late (August) growing season. Table 3 shows that G4 and G5 have a similar level of skill at reproducing the mean observed profiles over the campaign.

Table 3 also shows the mean model minus measurement statistics for INTEX-NA and YAK-AEROSIB. Generally, the model is within a 1.5 ppm of the measurements above the boundary layer with a standard deviation close to 3 ppm. The bias and

Title Page

Abstract

Introduction

Conclusions

References

Tables

Figures

◀

▶

◀

▶

Back

Close

Full Screen / Esc

Printer-friendly Version

Interactive Discussion



standard deviation are typically higher for boundary layer measurements. For INTEX-NA and YAK-AEROSIB data, G4 and G5 show comparable performance. On the basis of this comparison there is no conclusive evidence that the model is suffering from a significant error in stratosphere-troposphere exchange, as previously suggested by Palmer et al. (2008).

6.2 Trend and seasonal variations of tropospheric CO₂

We use data from GLOBALVIEW, the AIRS space-borne sensor, and from the CONTRAIL aircraft campaign (Table 1) to assess how well the model reproduces observed large-scale trends and latitude variability of CO₂.

6.2.1 Boundary layer

Figure 6 shows the GLOBALVIEW and model CO₂ concentration record from 2003 to 2006, inclusive, averaged over 30° latitude bins. To extract the trend and the seasonal cycle from surface CO₂ time series $f(t)$, we decompose $f(t)$ into polynomial and harmonic functions (Thoning et al., 1989) after smoothing with a 8-week moving average:

$$f(t) = a_0 + a_1 t + a_2 \sin(2\pi t) + a_3 \cos(2\pi t) + a_4 \sin(4\pi t) + a_5 \cos(4\pi t), \quad (4)$$

where t runs from 0 to 4 yr (i.e., from 2003 to 2006). The coefficient a_0 represents the mean, and a_1 is the annual trend. The amplitude of the seasonal cycle a_s is calculated by $a_s = \sqrt{a_2^2 + a_3^2}$.

Table 4 shows the GLOBALVIEW and G4/G5 model trend and seasonal cycles. For comparison, we also include the results for G4 model using the a priori surface flux estimates. For model evaluation we use GLOBALVIEW data from all 277 stations when it was available. The G4 model driven by a priori fluxes overestimates the trend by more than 100%. We generally find that the a posteriori fluxes are more consistent with the observed seasonal cycle, with differences typically less than 20%. We find that for all latitudes, the G4 and G5 model generally underestimates the annual trend

Title Page

Abstract

Introduction

Conclusions

References

Tables

Figures

◀

▶

◀

▶

Back

Close

Full Screen / Esc

Printer-friendly Version

Interactive Discussion



by 4–10%, mainly due to the possibly overestimated a posteriori terrestrial sink (as described above).

Figure 7 shows the latitudinal gradient of 2004 GLOBALVIEW surface CO₂ data, binned at 10° latitude intervals, is 0.033 ppm/° latitude over 60° S–60° N. The G4 and G5 model gradients for the same latitude range are 0.033 ppm/° latitude and 0.036 ppm/° latitude, respectively. G4 model zonal means agree to within 1 ppm of the GLOBALVIEW data at all extratropical latitudes, which increases to 1.5 ppm over the tropics where observations are sparse. G4 and G5 model zonal means are similar except between 30° N–50° N where the G5 model has a bias of of 1 ppm. The results for 2005 and 2006 (not shown) are similar.

6.2.2 Free troposphere

Figure 8 shows a time series of level-3 monthly mean AIRS data, averaged over 30° latitude bins. The G4 and G5 models have been sampled at the appropriate time and location of each gridded AIRS measurement, and convolved with a latitude-dependent AIRS weighting function (Chahine et al., 2008). AIRS CO₂ concentrations show a global trend of 2.21–2.63 ppm yr⁻¹ while the G4/G5 models have a trend of 1.95–2.19 ppm yr⁻¹.

Over southern high latitudes, AIRS data are not available; the model values have only a weak seasonal cycle as expected. Over southern middle latitudes the model has a smaller seasonal cycle and lower concentrations than observed by AIRS, suggesting errors in the fluxes and/or atmospheric transport.

Over northern tropical latitudes, the a posteriori model seasonal cycle is in good agreement with AIRS, but has an amplitude much smaller than the sparse GLOBALVIEW aircraft data that span 5–8 km. We did not observe the difference in seasonal cycle with the ground-based GLOBALVIEW data, suggesting that incorrect model vertical transport plays an important role in the discrepancy between the model and data. Over northern mid-latitudes, the model and AIRS seasonal cycles are of comparable magnitude but there is a phase shift with the model leading by 1–2 months which

Title Page

Abstract

Introduction

Conclusions

References

Tables

Figures

◀

▶

◀

▶

Back

Close

Full Screen / Esc

Printer-friendly Version

Interactive Discussion



is consistent with the sparse GLOBALVIEW aircraft observations which span 5–8 km. Previous work has also reported GEOS-Chem model bias in the seasonal cycle of CO₂ (Palmer et al., 2008), which has been attributed to deficiencies in modeling vertical transport in the free troposphere. We do not reproduce the AIRS seasonal cycle at northern high latitudes, with the model more consistent with the GLOBALVIEW data.

6.2.3 Upper troposphere and lower stratosphere

Figure 9a and b shows CONTRAIL and model CO₂ concentrations during 2003–2006. We sample the models at the time and location of each CONTRAIL measurement, and bin them between 35° S–0° and 0°–35° N between 8–13 km. The resulting model and observed trends are similar (2.00–2.15 ppm yr⁻¹) in both latitude bands. The models also capture the observed magnitude and phase of the seasonal cycle in both hemispheres. Figure 9c shows the CONTRAIL and model latitude gradient of CO₂ concentrations. Observed variations about the annual mean mainly reflect the seasonal cycles at 8–12 km, which have been slightly underestimated by our models. Coarse model horizontal resolution can also smear out small spatial variations shown in the neighbouring observations. At latitudes 15–30° N, model concentrations show much less variation than the observations: at 25° N, the observed variation is 2.4 ppm, while G4 (G5) model variation is only 1.4 ppm (1.1 ppm), partially due to transport deficiencies and coarse spatial resolutions. The G5 model has less variation than G4, suggesting that the G5 model has slower vertical mixing.

7 Conclusions

We have evaluated the GEOS-Chem model of atmospheric CO₂ using surface, aircraft and space-borne data. We have driven the model using GEOS-4 and GEOS-5 meteorology, which offers us an opportunity to assess the sensitivity of a posteriori fluxes to atmospheric transport, a priori fluxes of fossil fuel, biofuel, biomass burning, and

Title Page

Abstract

Introduction

Conclusions

References

Tables

Figures

◀

▶

◀

▶

Back

Close

Full Screen / Esc

Printer-friendly Version

Interactive Discussion



the terrestrial and ocean biospheres. Model analyses that used GEOS-4 and GEOS-5 meteorology are denoted by G4 and G5, respectively.

We fitted ocean (OC) and the sum of terrestrial biosphere (BS) and biomass burning (BB) CO₂ fluxes over 22 geographical regions to GLOBALVIEW surface data using an ensemble Kalman filter. Global annual BB+BS+OC CO₂ fluxes for G4 (G5) during 2004–2006 are -4.4 ± 0.9 (-4.2 ± 0.9), -3.9 ± 0.9 (-4.5 ± 0.9), and -5.2 ± 0.9 (-4.9 ± 0.9) Pg C yr⁻¹, respectively.

The large bias between G4 and G5 global estimated fluxes in 2005 result mainly from differences in G4 and G5 meteorology.

The sign and magnitude of regional a posteriori CO₂ fluxes are in broad agreement with TransCom 3 flux estimates for 1992–1996, but our model has a larger sink over northern and southern continents. The stronger drawdown during the growing season and weaker source during the rest of the year represents a substantial departure from the annually-balanced CASA model, possibly reflecting one or a combination of reasons, as found by previous studies, e.g., overestimating prior biospheric respiration, errors in prescribed fossil fuel emission, and errors in boundary layer transport.

We evaluated the a posteriori model vertical CO₂ profile against aircraft campaign data from COBRA 2004 (May–August), INTEX-NA (July–August), and YAK AEROSIB (April, September). The G4 and G5 models reproduced the mean observed concentrations in the free troposphere and upper troposphere generally within 1.5 ppm, with substantial variations that reflect sub-grid variability. However, we found the model had difficulty capturing boundary layer concentrations observed during COBRA during early (May) and late (August) growing season over North America. The a posteriori G4 and G5 surface concentration trend is 4–10% lower than GLOBALVIEW data, and the model seasonal cycles are within 20% of GLOBALVIEW. The observed latitude gradient of CO₂ over 60° S–60° N (0.033 ppm/°latitude) is well reproduced by the G4 and G5 model.

The model has a small negative bias in the free troposphere CO₂ trend (1.95–2.19 ppm yr⁻¹) compared to AIRS data which has a trend of 2.21–2.63 ppm yr⁻¹, con-

GEOS-Chem CO₂ simulation

L. Feng et al.

Title Page

Abstract

Introduction

Conclusions

References

Tables

Figures

◀

▶

◀

▶

Back

Close

Full Screen / Esc

Printer-friendly Version

Interactive Discussion



sistent with surface data. Over southern middle and tropical latitudes the model overestimates the seasonal cycle observed by AIRS. Over northern tropical latitudes the model seasonal cycle is in good agreement with AIRS. Over northern mid-latitudes the observed and model seasonal cycle are of comparable magnitude but the model leads AIRS by 1–2 months.

Model CO₂ concentrations in the upper troposphere reproduce the trend of about 2.0 ppm yr⁻¹ over 2003–2006 observed by CONTRAIL. The models also captures the observed mean latitude gradient, but both the CONTRAIL observations and models show significant variation about that mean particularly at latitudes greater than 10° N.

Based on our (limited) model evaluation we find no significant bias in GEOS model transport that would necessarily impede progress in quantitatively understanding major processes in the carbon cycle. However, we acknowledge that once we start evaluating model CO₂ concentrations above the boundary layer the data available quickly becomes sparse in time and space. Global space-borne tropospheric column measurements of CO₂, with the accuracy and precision required for surface CO₂ flux estimation, are fast becoming a reality. To establish and maintain confidence in these column measurements, we must start to strengthen column and in situ measurement capabilities that facilitate regular access to the free and upper troposphere over continents and over the remote troposphere without the constraints imposed by commercial air corridors. This can be and is being achieved using vehicles such as the Gulfstream V and the Globalhawk UAV that have the capability of duration flying in the free and upper troposphere.

Acknowledgements. We gratefully acknowledge the GLOBALVIEW project based at NOAA ESRL; Steve Wofsy (Harvard University) and the COBRA project funded principally by NASA; the CONTRAIL project team; and the engineers and scientists associated the NASA AIRS satellite instrument. This study is funded by the UK Natural Environment Research Council under NE/H003940/1. YY acknowledges funding from the China Scholarship Council.

**GEOS-Chem CO₂
simulation**

L. Feng et al.

Title Page

Abstract

Introduction

Conclusions

References

Tables

Figures

◀

▶

◀

▶

Back

Close

Full Screen / Esc

Printer-friendly Version

Interactive Discussion



References

- Bakwin, P. S., Tans, P. P., Stephens, B. B., Wofsy, S. C., Gerbig, C., and Grainger, A.: Strategies for measurement of atmospheric column means of carbon dioxide from aircraft using discrete sampling, *J. Geophys. Res.*, 108, 4514, doi:10.1029/2002JD003306, 2003. 18029, 18032
- 5 Bloom, S., da Silva, A., Dee, D., Bosilovich, M., Chern, J.-D., Pawson, S., Schubert, S., Sienkiewicz, M., Stajner, I., Tan, W.-W., and Wu, M.-L.: Documentation and Validation of the Goddard Earth Observing System (GEOS) Data Assimilation System – Version 4, Tech. Rep. Technical Report Series on Global Modeling and Data Assimilation 104606, 26, NASA Global Modeling and Assimilation Office, 2005. 18029
- 10 Chahine, M. T., Chen, L., Dimotakis, P., Jiang, X., Li, Q., Olsen, E. T., Pagano, T., Randerson, J., and Yung, Y. L.: Satellite remote sounding of mid-tropospheric CO₂, *Geophys. Res. Lett.*, 35, L17807, doi:10.1029/2008GL035022, 2008. 18033, 18041, 18060
- Erickson, D. J., Mills, R. T., Gregg, J., Blasing, T. J., Hoffman, F. M., Andres, R. J., Devries, M., Zhu, Z., and Kawa, S. R.: An estimate of monthly global emissions of anthropogenic CO: impact on the seasonal cycle of atmospheric CO₂, *J. Geophys. Res.*, 113, G01023, doi:10.1029/2007JG000435, 2008. 18030, 18037
- 15 Feng, L., Palmer, P. I., Bösch, H., and Dance, S.: Estimating surface CO₂ fluxes from spaceborne CO₂ dry air mole fraction observations using an ensemble Kalman filter, *Atmos. Chem. Phys.*, 9, 2619–2633, doi:10.5194/acp-9-2619-2009, 2009. 18034
- 20 GLOBALVIEW-CO₂: Cooperative Atmospheric Data Project Carbon Dioxide, CD-ROM, NOAA GMD, Boulder, Colorado (also available via anonymous FTP to ftp.cmdl.noaa.gov, path: ccg/co2/GLOBALVIEW), 2006. 18031
- Gurney, K. R., Baker, D., Rayner, P., and Denning, S.: Interannual variations in continental-scale net carbon exchange and sensitivity to observing networks estimated from atmospheric CO₂ inversions for the period 1980 to 2005, *Global Biogeochem. Cy.*, 22, GB3025, doi:10.1029/2007GB003082, 2008. 18034, 18035
- 25 Gurney, K. R., Law, R. M., Denning, A. S., et al.: Towards robust regional estimates of CO₂ sources and sinks using atmospheric transport models, *Nature*, 415, 626–630, 2002. 18028, 18030, 18033
- 30 Gurney, K. R., Law, R. M., Denning, A. S., et al.: TransCom 3 inversion intercomparison: 1. Annual mean control results and sensitivity to transport and prior flux information, *Tellus B*, 55, 555–579, 2003. 18028, 18032, 18034, 18037, 18050

GEOS-Chem CO₂ simulation

L. Feng et al.

Title Page

Abstract

Introduction

Conclusions

References

Tables

Figures

◀

▶

◀

▶

Back

Close

Full Screen / Esc

Printer-friendly Version

Interactive Discussion



**GEOS-Chem CO₂
simulation**

L. Feng et al.

Title Page

Abstract

Introduction

Conclusions

References

Tables

Figures

◀

▶

◀

▶

Back

Close

Full Screen / Esc

Printer-friendly Version

Interactive Discussion



- Gurney, K. R., Law, R. M., Denning, A. S., et al.: Transcom 3 inversion intercomparison: model mean results for the estimation of seasonal carbon sources and sinks, *Global Biogeochem. Cy.*, 18, GB1010, doi:10.1029/2003GB002111, 2004. 18028, 18034, 18036, 18037, 18053
- 5 Heald, C. L., Jacob, D. J., Jones, D. B. A., Palmer, P. I., Logan, J. A., Streets, D. G., Sachse, G. W., Gille, J. C., Hoffman, R. N., and Nehrkorn, T.: Comparative inverse analysis of satellite (MOPITT) and aircraft (TRACE-P) observations to estimate Asian sources of carbon monoxide, *J. Geophys. Res.*, 109, D23306, doi:10.1029/2004JD005185, 2004. 18028
- Li, Q., Palmer, P. I., Pumphrey, H. C., Bernath, P., and Mahieu, E.: What drives the observed variability of HCN in the troposphere and lower stratosphere?, *Atmos. Chem. Phys.*, 9, 8531–8543, doi:10.5194/acp-9-8531-2009, 2009. 18028
- 10 Li, Q. B., Jacob, D. J., Yantosca, R. M., Heald, C. L., Singh, H. B., Koike, M., Zhao, Y., Sachse, G. W., and Streets, D. G.: A global 3-D model evaluation of the atmospheric budgets of HCN and CH₃CN: constraints from aircraft measurements over the Western Pacific, *J. Geophys. Res.*, 108, 8827, doi:10.1029/2002JD003075, 2003. 18028
- Marland, G., Boden, T. A., and Andres, R. J.: Global, regional, and national CO₂ emissions, in: Trends: A Compendium of Data on Global Change, Tech. Rep. 2007. 7346, Carbon Dioxide Information Analysis Center Oak Ridge National Laboratory, US Department of Energy, Oak Ridge, Tenn., USA, 2007. 18030
- 20 Masarie, K. A. and Tans, P. P.: Extension and integration of atmospheric carbon dioxide data into a globally consistent measurement record, *J. Geophys. Res.*, 100, 522–529, 1995. 18032
- Matsueda, H., Inoue, H. Y., and Ishii, M.: Aircraft observation of carbon dioxide at 8–13 km altitude over the Western Pacific from 1993 to 1999, *Tellus B*, 54, 1–21, 2002. 18032
- 25 Olsen, S. C. and Randerson, J. T.: Differences between surface and column atmospheric CO₂ and implications for carbon cycle research, *J. Geophys. Res.*, 109, D02301, doi:10.1029/2003JD003968, 2004. 18031
- Palmer, P. I., Suntharalingam, P., Jones, D. B. A., Jacob, D. J., Streets, D. G., Fu, Q., Vay, S. A., and Sachse, G. W.: Using CO₂:CO correlations to improve inverse analyses of carbon fluxes, *J. Geophys. Res.*, 111, D12318, doi:10.1029/2005JD006697, 2006. 18030, 18031, 18035
- 30 Palmer, P. I., Barkley, M. P., and Monks, P. S.: Interpreting the variability of space-borne CO₂ column-averaged volume mixing ratios over North America using a chemistry transport

**GEOS-Chem CO₂
simulation**

L. Feng et al.

Title Page

Abstract

Introduction

Conclusions

References

Tables

Figures

◀

▶

◀

▶

Back

Close

Full Screen / Esc

Printer-friendly Version

Interactive Discussion



model, *Atmos. Chem. Phys.*, 8, 5855–5868, doi:10.5194/acp-8-5855-2008, 2008. 18028, 18030, 18035, 18040, 18042

Paris, J.-D., Ciais, P., Nedelec, P., Ramonet, M., Belan, B. D., Arshinov, M. Y., Golitsyn, G. S., Granberg, I., Stohl, A., Cayez, G., Athier, G., Bournard, F., and Cousin, J. M.: The YAK-AEROSIB transcontinental aircraft campaigns: new insights on the transport of CO₂, CO, and O₃ across Siberia, *Tellus B*, 60, 551–568, 2008. 18032

Paris, J.-D., Ciais, P., Nedelec, P., Stohl, A., Belan, B. D., Arshinov, M. Y., Carouge, C., Golitsyn, G. S., and Granberg, I. G.: New insights on the chemical composition of the Siberian air shed from the YAK-AEROSIB aircraft campaigns, *B. Am. Meteorol. Soc.*, 91(5), 625–641, 2010. 18032

Phillips, O. L., Aragao, L. E. O. C., Lewis, S. L., Fisher, J. B., Lloyd, J., Lopez-Gonzalez, G., Malhi, Y., Monteagudo, A., Peacock, J., Quesada, C. A., van der Heijden, G., Almeida, S., Amaral, I., Arroyo, L., Aymard, G., Baker, T. R., Banki, O., Blanc, L., Bonal, D., Brando, P., Chave, J., Alves de Oliveira, A. C., Cardozo, N. D., Czimczik, C. I., Feldpausch, T. R., Freitas, M. A., Gloor, E., Higuchi, N., Jimenez, E., Lloyd, G., Meir, P., Mendoza, C., Morel, A., Neill, D. A., Nepstad, D., Patino, S., Cristina Penuela, M., Prieto, A., Ramirez, F., Schwarz, M., Silva, J., Silveira, M., Thomas, A. S., ter Steege, H., Stropp, J., Vasquez, R., Zelazowski, P., Alvarez Davila, E., Andelman, S., Andrade, A., Chao, K.-J., Erwin, T., Di Fiore, A., Honorio C, E., Keeling, H., Killeen, T. J., Laurance, W. F., Pena Cruz, A., Pitman, N. C. A., Nunez Vargas, P., Ramirez-Angulo, H., Rudas, A., Salamao, R., Silva, N., Terborgh, J., and Torres-Lezama, A.: Drought sensitivity of the Amazon rainforest, *Science*, 323, 1344–1347, 2009. 18038

Randerson, J. T., Thompson, M. V., Conway, T. J., Fung, I. Y., and Field, C. B.: The contribution of terrestrial sources and sinks to trends in the seasonal cycle of atmospheric carbon dioxide, *Global Biogeochem. Cy.*, 11, 535–560, 1997. 18031

Rienecker, M., Suarez, M. R., Todling, J. B., Takacs, L., Liu, H.-C., Gu, W., Sienkiewicz, M., Koster, R., Gelaro, R., Stajner, I., and Nielsen, J.: The GEOS-5 Data Assimilation System – Documentation of Versions 5.0.1, 5.1.0, and 5.2.0, Tech. Rep. Technical Report Series on Global Modeling and Data Assimilation, 27, NASA Global Modeling and Assimilation Office, <http://gmao.gsfc.nasa.gov/pubs/tm/>, (last access: May 2010), 2008. 18029

Rödenbeck, C., Houweling, S., Gloor, M., and Heimann, M.: CO₂ flux history 1982–2001 inferred from atmospheric data using a global inversion of atmospheric transport, *Atmos. Chem. Phys.*, 3, 1919–1964, doi:10.5194/acp-3-1919-2003, 2003. 18028

**GEOS-Chem CO₂
simulation**

L. Feng et al.

Title Page

Abstract

Introduction

Conclusions

References

Tables

Figures

◀

▶

◀

▶

Back

Close

Full Screen / Esc

Printer-friendly Version

Interactive Discussion



- Shia, R. L., Liang, M.-C., Miller, C. E., and Yung, Y. L.: CO₂ in the upper troposphere: influence of stratosphere-troposphere exchange, *Geophys. Res. Lett.*, 33, L14814, doi:10.1029/2006GL026141, 2006. 18029
- 5 Singh, H. B., Brune, W. H., Crawford, J. H., Jacob, D. J., and Russell, P. B.: Overview of the summer 2004 Intercontinental Chemical Transport Experiment North America (INTEX-A), *J. Geophys. Res.*, 111, D24S01, doi:10.1029/2006JD007905, 2006. 18032
- Stephens, B., Gurney, K. R., Tans, P., et al.: Weak northern and strong tropical land carbon uptake from vertical profiles of atmospheric CO₂, *Science*, 316, 5832, doi:10.1126/Science.113704, 2007. 18028, 18036, 18037
- 10 Suntharalingam, P., Randerson, J. T., Krakauer, N., Jacob, J. D., and Logan, J. A.: The influence of reduced carbon emissions and oxidation on the distribution of atmospheric CO₂: implications for inversion analysis, *Global Biogeochem. Cy.*, 19, GB4003, doi:10.1029/2005GB002466, 2005. 18030, 18031
- Takahashi, T., Sutherland, S. C., Wanninkhof, R., et al.: Global sea-air CO₂ flux based on climatological surface ocean pCO₂, and seasonal biological and temperature effects, *Deep-Sea Res. Pt. II*, 49, 1601–1622, 2009. 18030
- 15 Thoning, K. W., Tans, P. P., and Komhyr, W. D.: Atmospheric carbon dioxide at Mauna Loa Observatory: 2. Analysis of the NOAA GMCC data, 1974–1985, *J. Geophys. Res.*, 94, 8549–8565, 1989. 18040
- 20 van der Werf, G. R., Randerson, J. T., Giglio, L., Collatz, G. J., Kasibhatla, P. S., and Arellano Jr., A. F.: Interannual variability in global biomass burning emissions from 1997 to 2004, *Atmos. Chem. Phys.*, 6, 3423–3441, doi:10.5194/acp-6-3423-2006, 2006. 18030
- Yang, Z. R. A. W., Keppel-Aleks, G., Krakauer, N. Y., Randerson, J. T., Tans, P. P., Sweeney, C., and Wennberg, P. O.: New constraints on Northern Hemisphere growing season net flux, *Geophys. Res. Lett.*, 34, L12807, doi:10.1029/2007GL029742, 2007. 18028
- 25 Yevich, R. and Logan, J. A.: An assessment of biofuel use and burning of agricultural waste in the developing world, *Global Biogeochem. Cy.*, 17, 1095, doi:10.1029/2002GB001952, 2003. 18030

GEOS-Chem CO₂ simulation

L. Feng et al.

Table 1. Summary of the geographical region, time, and altitudes covered by the CONTRAIL, COBRA, INTEX-NA, and YAK-AEROSIB aircraft CO₂ concentration measurements.

Name	Region	Period	Altitude [km]
CONTRAIL	Western Pacific (140°–149° E, 30° S–33° N)	1993–present	8–13
COBRA (2004)	Eastern North America (65°–106° W, 40°–50° N)	May–Aug 2004	0–11
INTEX-NA	North America (36° W–139° W, 27° N–53° N)	Jul–Aug 2004	0–12
YAK-AEROSIB	Siberia (80°–130° E, 55°–63° N)	11–14 Apr 2006; 7–10 Sep 2006	0–7

[Title Page](#)
[Abstract](#)
[Introduction](#)
[Conclusions](#)
[References](#)
[Tables](#)
[Figures](#)
[I◀](#)
[▶I](#)
[◀](#)
[▶](#)
[Back](#)
[Close](#)
[Full Screen / Esc](#)
[Printer-friendly Version](#)
[Interactive Discussion](#)


GEOS-Chem CO₂ simulation

L. Feng et al.

Title Page

Abstract

Introduction

Conclusions

References

Tables

Figures

◀

▶

◀

▶

Back

Close

Full Screen / Esc

Printer-friendly Version

Interactive Discussion



Table 2. A priori and a posteriori annual CO₂ flux estimates for BB+BS+OC (Pg C yr⁻¹) from north, tropical and south continental, and north, tropical and south oceans. The fourth column is the mean fluxes taken from the TransCom-3 experiments (Gurney et al., 2003) for 1992–1996.

Region	A priori	A posteriori G4 (G5)	TransCom-3
South continents	0.65	−0.46 (−0.43)	0.20
Tropical continents	1.26	0.80 (1.02)	1.10
North continents	0.21	−3.00 (−3.65)	−2.30
South ocean	−1.10	−1.56 (−1.41)	−1.10
Tropical ocean	0.69	0.56 (0.72)	0.40
North ocean	−0.96	−1.05 (−0.77)	−1.10

GEOS-Chem CO₂ simulation

L. Feng et al.

Title Page

Abstract

Introduction

Conclusions

References

Tables

Figures

◀

▶

◀

▶

Back

Close

Full Screen / Esc

Printer-friendly Version

Interactive Discussion



Table 3. The mean statistics of model minus CO₂ measurements (ppm) for the COBRA, INTEX-NA, and YAK-AEROSIB aircraft campaigns.

Altitude (km)	G4 COBRA (G5)		G4 INTEX-NA (G5)		G4 YAK-AEROSIB (G5)	
	Mean	Std	Mean	Std	Mean	Std
0–2	0.59 (0.53)	6.8 (7.4)	1.95 (1.54)	5.7 (5.7)	0.13 (–0.4)	2.6 (2.7)
2–8	1.06 (1.14)	2.9 (2.7)	1.01 (0.68)	2.1 (2.1)	–1.52 (–1.51)	1.7 (1.6)
8–12	0.47 (0.14)	1.3 (1.5)	1.22 (0.64)	1.9 (2.2)	N/A	N/A

**GEOS-Chem CO₂
simulation**

L. Feng et al.

Table 4. GLOBALVIEW and model trend a_1 (ppm yr⁻¹) and amplitude of the seasonal cycles a_s (ppm) in CO₂ concentrations in the boundary layers at six 30° latitude bands over 2004–2006.

Lat	GLOBALVIEW		G4 A posteriori (G5)		A priori	
	a_1	a_s	a_1	a_s	a_1	a_s
-75	1.91	0.54	1.86 (1.88)	0.49 (0.61)	4.40	0.87
-45	2.00	0.43	1.88 (1.90)	0.42 (0.48)	4.40	0.80
-15	1.97	0.31	1.92 (1.88)	0.31 (0.23)	4.35	0.23
15	2.14	3.27	2.07 (2.00)	3.30 (3.20)	4.29	2.93
45	2.25	5.62	2.21 (2.16)	5.65 (5.87)	4.28	5.57
75	2.43	6.77	2.38 (2.20)	6.90 (6.90)	4.43	6.50

[Title Page](#)
[Abstract](#)
[Introduction](#)
[Conclusions](#)
[References](#)
[Tables](#)
[Figures](#)
[I◀](#)
[▶I](#)
[◀](#)
[▶](#)
[Back](#)
[Close](#)
[Full Screen / Esc](#)
[Printer-friendly Version](#)
[Interactive Discussion](#)


GEOS-Chem CO₂ simulation

L. Feng et al.

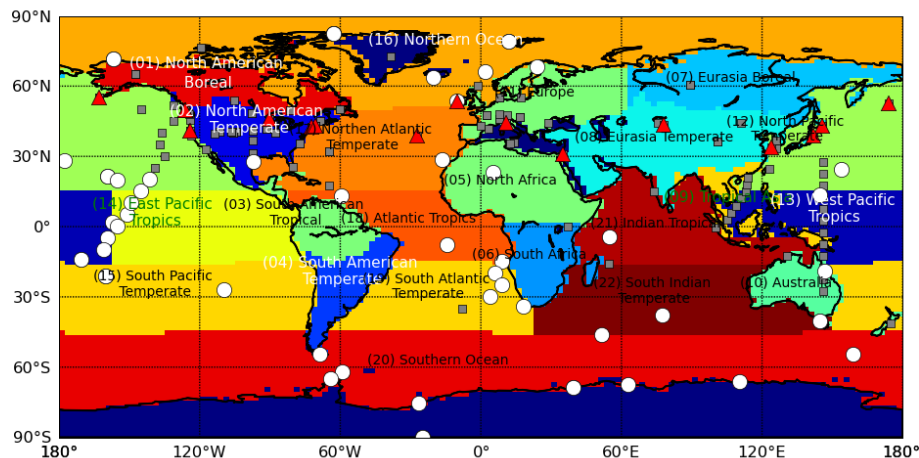


Fig. 1. The geographical distribution of 22 regions, based on the TransCom-3 study (Gurney et al., 2004), where we estimate CO₂ fluxes. The symbols denote the 277 GLOBALVIEW stations available during 2003–2006. The white circles are boundary layer stations with relative weights larger than 6 in 2005, and red triangles are mid-latitude stations (30–60° N) with relative weights larger than 4.0.

[Title Page](#)
[Abstract](#)
[Introduction](#)
[Conclusions](#)
[References](#)
[Tables](#)
[Figures](#)
[◀](#)
[▶](#)
[◀](#)
[▶](#)
[Back](#)
[Close](#)
[Full Screen / Esc](#)
[Printer-friendly Version](#)
[Interactive Discussion](#)

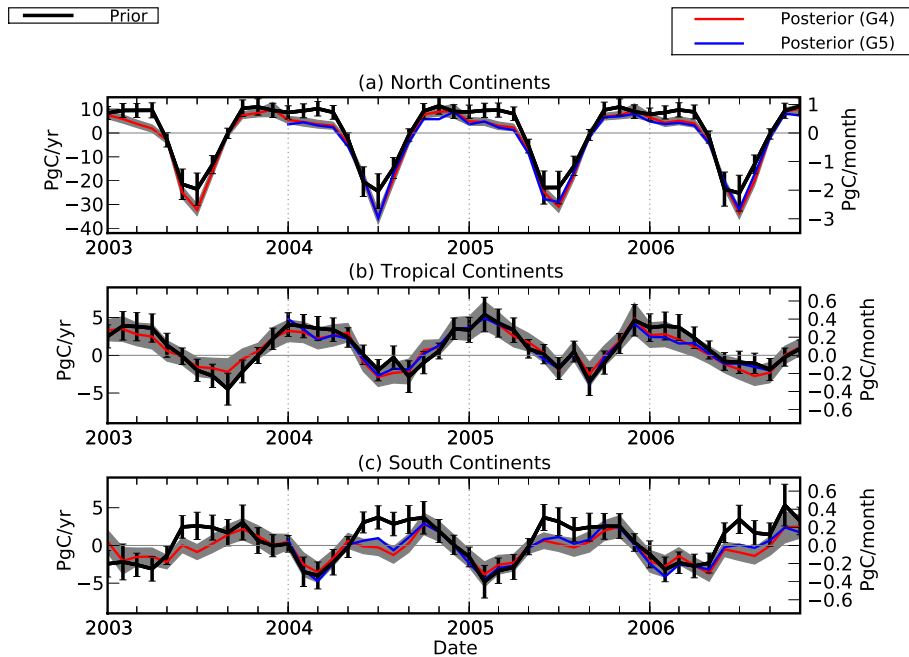



Fig. 2. Monthly mean GEOS-Chem a priori and a posteriori model CO_2 fluxes (Pg C month^{-1}) over 2003–2006, expressed also as the annual flux equivalent (Pg C yr^{-1}), averaged over the northern extratropical continents, the tropical continents, and the southern extratropical continents. The black line denotes the a priori estimates, with its uncertainty denoted by the vertical lines. The red line denotes the posteriori flux estimates after the GEOS-Chem model, driven by GEOS-4 (G4) meteorology, has been fitted to a subset of GLOBALVIEW station data using an ensemble Kalman filter, with the grey envelope denoting the a posteriori uncertainty. The blue line corresponds to the a posteriori flux estimates using GEOS-5 (G5) meteorological data.

GEOS-Chem CO_2 simulation

L. Feng et al.

Title Page	
Abstract	Introduction
Conclusions	References
Tables	Figures
◀	▶
◀	▶
Back	Close
Full Screen / Esc	
Printer-friendly Version	
Interactive Discussion	



GEOS-Chem CO₂ simulation

L. Feng et al.

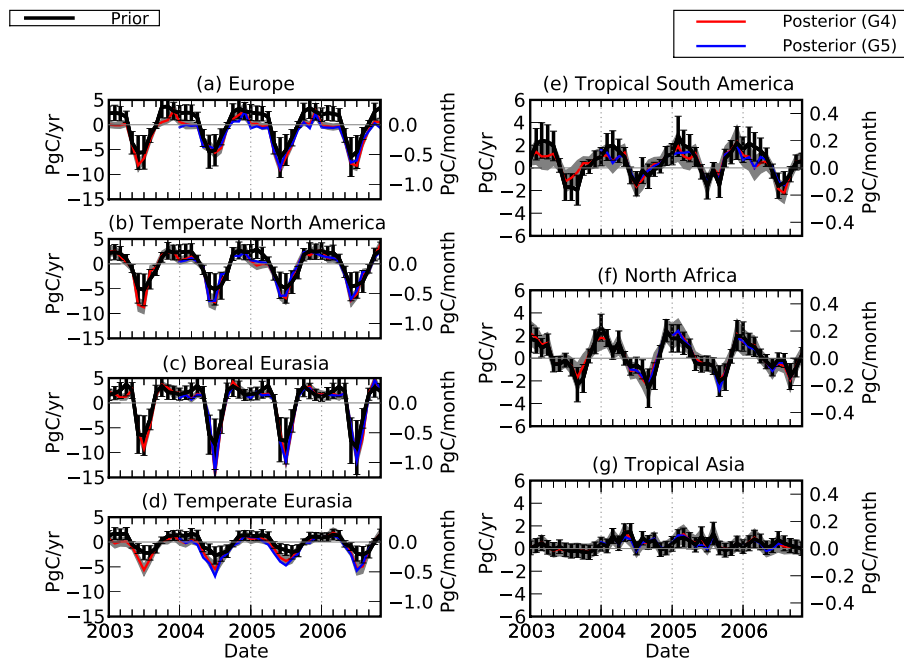


Fig. 3. Same as Fig. 2, but averaged over Europe, temperate North America, Boreal Eurasia, Temperate Eurasia, Tropical South America, Tropical North Africa, and Tropical Asia.

[Title Page](#)
[Abstract](#)
[Introduction](#)
[Conclusions](#)
[References](#)
[Tables](#)
[Figures](#)
[◀](#)
[▶](#)
[◀](#)
[▶](#)
[Back](#)
[Close](#)
[Full Screen / Esc](#)
[Printer-friendly Version](#)
[Interactive Discussion](#)


GEOS-Chem CO₂
simulation

L. Feng et al.

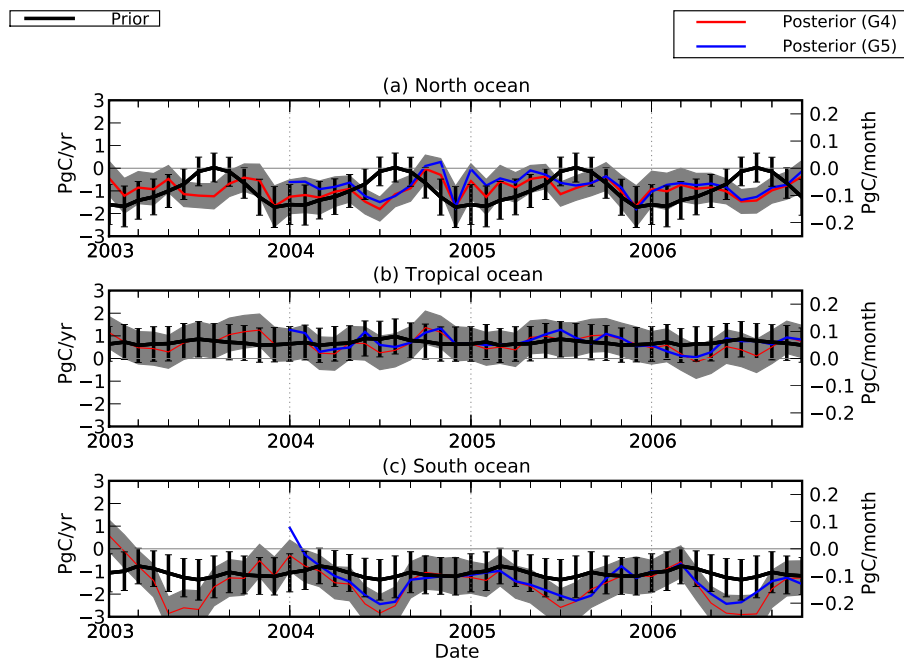


Fig. 4. Same as Fig. 2, but averaged over the northern extratropical oceans, the tropical oceans, and the southern extratropical oceans.

[Title Page](#)[Abstract](#)[Introduction](#)[Conclusions](#)[References](#)[Tables](#)[Figures](#)[◀](#)[▶](#)[◀](#)[▶](#)[Back](#)[Close](#)[Full Screen / Esc](#)[Printer-friendly Version](#)[Interactive Discussion](#)

GEOS-Chem CO₂
simulation

L. Feng et al.

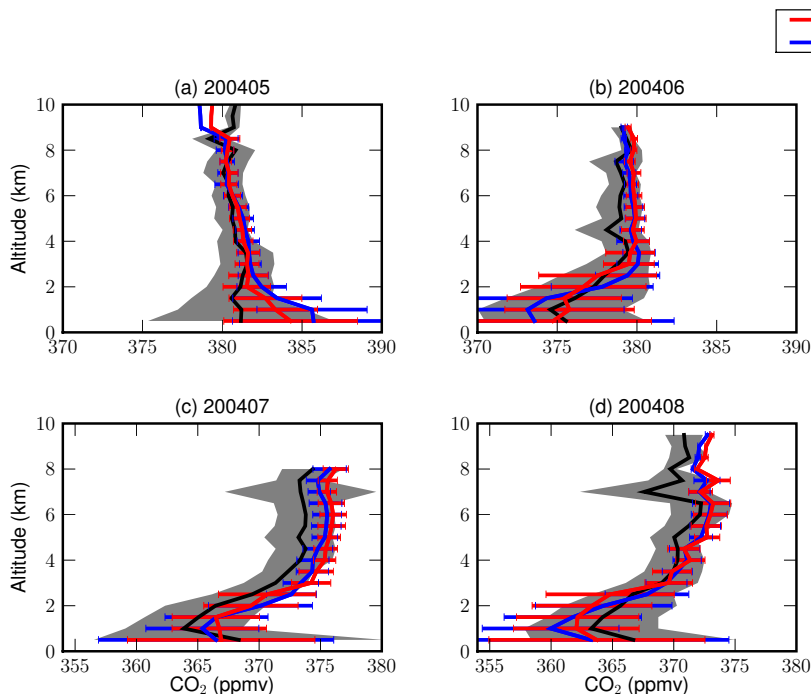


Fig. 5. Observed and GEOS-Chem a posteriori model CO₂ vertical profiles (ppm) taken from the CO₂ Budget and Regional Airborne Study over the Eastern North America averaged over (a) May, (b) June, (c) July, and (d) August 2004. The GEOS-Chem model, described at a horizontal resolution of $2 \times 2.5^\circ$, has been sampled at the time and location of each measurement. Data and model concentrations have been averaged over 500 m intervals. Monthly mean observations are denoted by the black lines, with the grey envelope representing the 1-standard deviation about that mean. Blue and red lines denote the monthly mean CO₂ concentrations corresponding to the G4 and G5 a posteriori flux estimates, respectively. The horizontal lines about a posteriori concentrations denote the 1-standard deviation about the monthly mean.

Title Page

Abstract

Introduction

Conclusions

References

Tables

Figures

◀

▶

◀

▶

Back

Close

Full Screen / Esc

Printer-friendly Version

Interactive Discussion



GEOS-Chem CO₂ simulation

L. Feng et al.

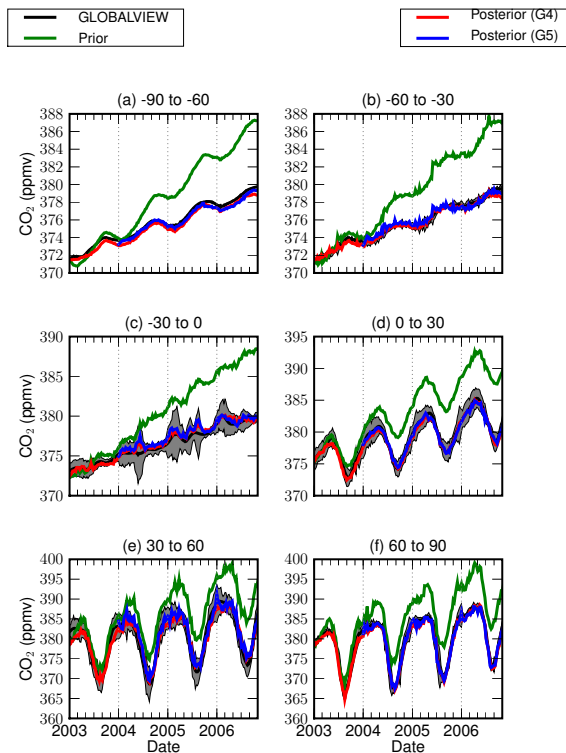


Fig. 6. GLOBALVIEW and GEOS-Chem a priori and a posteriori model CO₂ concentrations averaged over 30° latitude bins during 2003–2006: **(a)** 60–90° S, **(b)** 30–60° S, **(c)** 0–30° S, **(d)** 0–30° N, **(e)** 30–60° N, and **(f)** 60–90° N. Black lines denote the weekly mean GLOBALVIEW data at the latitude bins, with the grey envelope representing the 1-standard deviation about the mean. The GEOS-Chem model, described at a horizontal resolution of 2×2.5°, has been sampled at the time and location of each measurement. Green, red and blue lines denote the model weekly mean concentrations using a priori flux estimates, and a posteriori fluxes inferred using GEOS-4 (G4) and GEOS-5 (G5) meteorological fields, respectively.

[Title Page](#)
[Abstract](#)
[Introduction](#)
[Conclusions](#)
[References](#)
[Tables](#)
[Figures](#)
[◀](#)
[▶](#)
[◀](#)
[▶](#)
[Back](#)
[Close](#)
[Full Screen / Esc](#)
[Printer-friendly Version](#)
[Interactive Discussion](#)


GEOS-Chem CO₂
simulation

L. Feng et al.

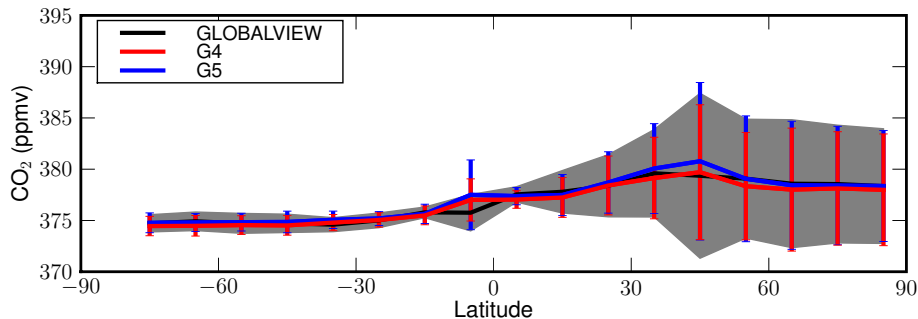


Fig. 7. Mean GLOBALVIEW (black) and GEOS-Chem a posteriori model (red G4 and blue G5) latitude gradients of CO₂ during 2004 binned at a resolution of 10°. The GEOS-Chem model, described at a horizontal resolution of 2×2.5°, has been sampled at the time and location of each measurement. The grey envelope describes the 1-standard deviation about the annual mean GLOBALVIEW surface CO₂ in the latitude bin, while vertical red (blue) lines correspond to G4 (G5) simulation.

[Title Page](#)[Abstract](#)[Introduction](#)[Conclusions](#)[References](#)[Tables](#)[Figures](#)[◀](#)[▶](#)[◀](#)[▶](#)[Back](#)[Close](#)[Full Screen / Esc](#)[Printer-friendly Version](#)[Interactive Discussion](#)

GEOS-Chem CO₂ simulation

L. Feng et al.

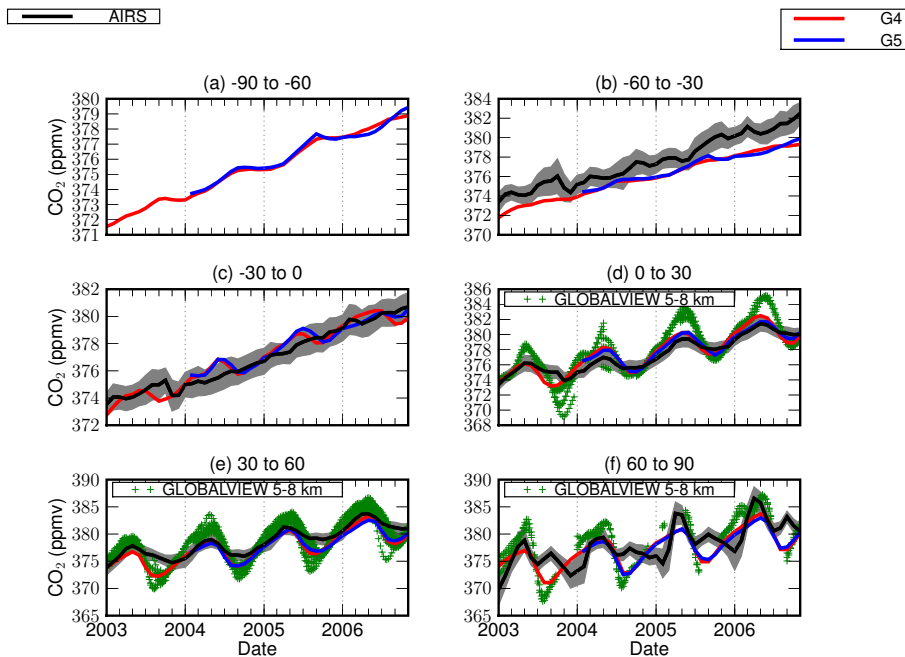


Fig. 8. Monthly-mean AIRS (black) and a posteriori model (red GEOS-4 and blue GEOS-5) CO₂ concentrations (ppmv) averaged over 30° latitude bins during 2003–2006: **(a)** 60–90° S, **(b)** 30–60° S, **(c)** 0–30° S, **(d)** 0–30° N, **(e)** 30–60° N, and **(f)** 60–90° N. The GEOS-Chem model, described at a horizontal resolution of 2×2.5°, has been sampled at the time and location of each AIRS level-3 CO₂ scene, weighted by the observation numbers, and convolved using the vertical weighting functions from Chahine et al. (2008). The grey envelope denote the 1-standard deviation about the zonal mean CO₂ observations in the latitude band. The green crosses are GLOBALVIEW aircraft measurements at vertical range 5–8 km.

[Title Page](#)
[Abstract](#)
[Introduction](#)
[Conclusions](#)
[References](#)
[Tables](#)
[Figures](#)
[◀](#)
[▶](#)
[◀](#)
[▶](#)
[Back](#)
[Close](#)
[Full Screen / Esc](#)
[Printer-friendly Version](#)
[Interactive Discussion](#)


GEOS-Chem CO₂ simulation

L. Feng et al.

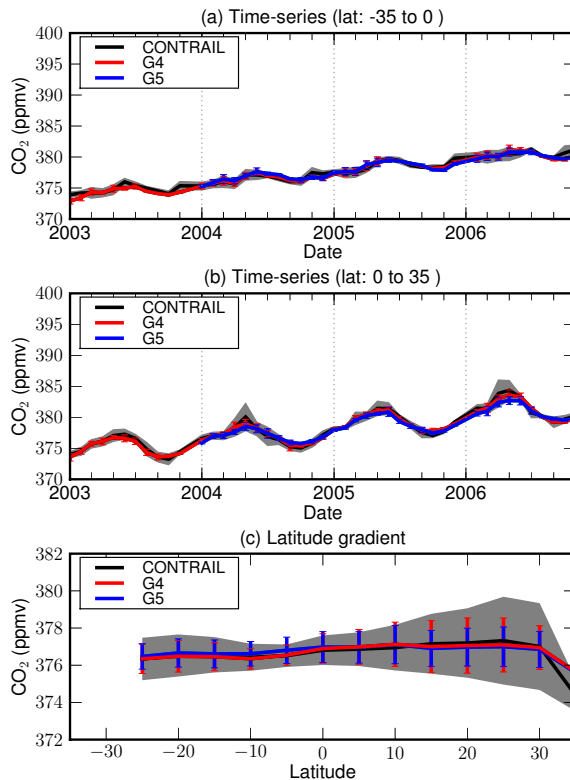


Fig. 9. Timeseries and latitude gradients of CONTRAIL (black) and GEOS-Chem a posteriori model (red G4 and blue G5) CO₂ concentrations (ppm). The model, described at a horizontal resolution of $2 \times 2.5^\circ$, has been sampled at the time of locations of each observation. The model and observed timeseries are averaged over (a) $0\text{--}35^\circ\text{S}$ and (b) $0\text{--}35^\circ\text{N}$ during 2003–2006. The model and observed latitude gradients (c) are averaged over 2004, with data binned at a 5° resolution. The grey envelope, and red and blue vertical lines denote the 1-standard deviation about the mean CONTRAIL, G4, and G5 model CO₂ concentrations, respectively.

[Title Page](#)
[Abstract](#)
[Introduction](#)
[Conclusions](#)
[References](#)
[Tables](#)
[Figures](#)
[◀](#)
[▶](#)
[◀](#)
[▶](#)
[Back](#)
[Close](#)
[Full Screen / Esc](#)
[Printer-friendly Version](#)
[Interactive Discussion](#)
